ISSN (Print) 1226-1750
ISSN (Online) 2233-6656
Journal of Magnetics 25(2), 307-312 (2020) https://doi.org/10.4283/JMAG.2020.25.2.307

Magnetized Darcy-Forchheimer Stagnation Point Flow of Micropolar Ferrosoferric Oxide Fluid with Velocity Slip and Convective Boundary Condition

M. Ijaz Khan[1]*, Seifedine Kadry[2], Yu-Ming Chu[3,4]*, El Mostafa Kalmoun[5], and Zulfiqar Ali[1]

[1]*Department of Mathematics, Riphah International University, Faisalabad Campus, Faisalabad 38000, Pakistan*
[2]*Department of Mathematics and Computer Science, Beirut Arab University, Beirut, Lebanon*
[3]*Department of Mathematics, Huzhou University, Huzhou 313000, P. R. China*
[4]*Hunan Provincial Key Laboratory of Mathematical Modeling and Analysis in Engineering, Changsha University of Science & Technology, Changsha 410114, P. R. China*
[5]*Department of Mathematics, Statistics and Physics, College of Arts and Sciences, Qatar University*

(Received 17 May 2020, Received in final form 21 June 2020, Accepted 23 June 2020)

The present communication develops the governing expressions that describe a steady incompressible two-dimensional flow of micropolar Ferrosoferric Oxide fluid towards a stretched surface under the impact of Lorentz force (magnetic field). Ferrofluids are made out of nanoscale ferromagnetic materials suspended in a base fluid (oil, kerosene, water). The distinction between the magnetorheological fluids (MRF) and ferrofluids (FF) is the size of the materials. The materials in a ferrofluid fundamentally comprise of nanomaterials, which are suspended by Brownian diffusion and generally under normal conditions will not settle. Here, Ferrosoferric Oxide (Fe_3O_4) is considered as nanoparticle and water as a base fluid. The governing equations are modeled by using Tiwari-Das nanofluid model with the help of appropriate similarity transformations. Furthermore, radiative heat flux and convective boundary condition is accounted. The numerical results of the governing equations are obtained through implementation of Built-in-Shooting technique. The impact of radiation parameter, stretching ratio parameter, magnetic parameter, thermal Biot number, micro-rotation parameter, velocity slip parameter and Darcy-Forchheimer number on the flow velocity and temperature are revealed graphically and discussed. The engineering curiosity like skin friction and Nusselt number are computationally computed and tabulated.

Keywords : darcy-forchheimer porous medium, micropolar ferrosoferric oxide fluid, convective boundary condition, radiative heat flux, stagnation point flow, velocity slip

1. Introduction

For the last several years, many scientists have been strongly attracted towards the problems involving non-Newtonian flow. Due to their significant characteristics, the flow analysis with different geometries has many applications, for instance, electronic equipment, cooling applications in atomic reactors and several other hydrodynamics processes. Moreover, the flow analysis of nanofluids has many significant applications in the industrial sectors, such as, drawing of plastic films, production paper, manufacturing of glass and crude oil refineries etc. In addition to this, the implementation of the nanotechnology has been an aim of the recent analysis by many scholars for their remarkable electrical, optical, chemical uses. Owing to such features, these nanoparticles are also used in catalysis, imaging, energy-based research, micro-electronics, medical and environmental applications. These particles are composed of metals or non-metals. On top of that, latest investigations have made the in-fusion of nanoparticles, practicable in heat transfer fluids most notably water, diethylene glycol and propylene glycol to convert them into a more efficient category of heat transfer fluids [1]. Nanofluids are actually the suspension of nanoparticles in a base fluid. These fluids have higher thermal conductivity and significant characteristics as compare to conventional fluids. Many attempts have been made by taking different aspects of the flows [2-12].

The second law of thermodynamics states that the

*Co-corresponding author: Tel: +92-335-9761475
Fax: +92-335-9761475, e-mail: ijazfmg_khan@yahoo.com
e-mail: chuyuming@zjhu.edu.cn

entropy of any system will tend to increase. Intuitively speaking, the term entropy measures the disturbance in a system. It is caused by the irreversibility in physical life problems. In real-world applications, it is needed to increase the efficiency of machines by reducing the irreversibility effects in the system. That is why entropy optimization and Bejan number are more emphasized in this article. The dimensionless Bejan number is determined to measure the ratio of thermal to total irreversibilities. This number exists between 0 and 1. Numerous attempts have been done on this regards by taking different aspects of the entropy optimized flows [13-25].

The main target of this research communication is to adopt the Built-in-Shooting method [26] for examining the impact of magnetized Darcy-Forchheimer stagnation point of micropolar Ferrosoferric Oxide fluid with the convective boundary condition and velocity slip towards a stretched surface. The flow is electrically conducted with the help of applied magnetic field and generated due to stretching phenomenon. Furthermore, the energy equation is developed with the help of law of conservation of energy. The pertinent flow parameters are graphically discussed.

2. Mathematical Description and Coordinate System

Here governing equations are developed for the steady, incompressible 2D micropolar Ferrosoferric Oxide fluid flow by a stretchable surface of the sheet. The flow is caused by slip and stretching phenomenon and saturated and electrically conducting through Darcy-Forchheimer relation and applied magnetic field of strength (B_0). Furthermore, convective boundary condasion is also considered at the boundary. Let $u_w = ax$ highlights the stretching velocity, $u_{slip} = \gamma_1 \frac{\partial u}{\partial y}$ the velocity slip, $v = 0$ indicates there is no suction/injection, $N = -m_0 \frac{\partial u}{\partial y}$ illustrates the micro-rotation along with boundary parameter, T, T_∞ respectively the surface or fluid and ambient temperature respectively. Under the above assumptions the governing equations are

$$\frac{\partial u}{\partial x} + \frac{\partial v}{\partial y} = 0, \tag{1}$$

$$\left.\begin{aligned} u\frac{\partial u}{\partial x} + v\frac{\partial u}{\partial y} = u_e \frac{du_e}{dx} + \frac{(\mu_{nf}+\kappa^*)}{\rho_{nf}}\frac{\partial^2 u}{\partial y^2} + \frac{\kappa^*}{\rho_{nf}}\frac{\partial N}{\partial y} - \frac{\sigma_{nf}}{\rho_{nf}}B_0^2(u-u_e) \\ + g\frac{(\beta_1\rho)_{nf}}{\rho_{nf}}(T-T_\infty) - \frac{\nu_{nf}}{K^*}(u-u_e) - F(u^2-u_e^2), \end{aligned}\right\} \tag{2}$$

$$u\frac{\partial N}{\partial x} + v\frac{\partial N}{\partial y} = \frac{\gamma_{nf}}{\rho_{nf} j}\frac{\partial^2 N}{\partial y^2} - \frac{\kappa^*}{\rho_{nf} j}\left(2N + \frac{\partial u}{\partial y}\right), \tag{3}$$

$$u\frac{\partial T}{\partial x} + v\frac{\partial T}{\partial y} = \frac{1}{(\rho c_p)_{nf}}\left(k_{nf} + \frac{16\sigma^\circ T_\infty^3}{3k^\circ}\right)\frac{\partial^2 T}{\partial y^2}, \tag{4}$$

with

$$\left.\begin{aligned} u = U_w + U_{slip},\ v = 0,\ N = -m_0\frac{\partial u}{\partial y}, -k_f\frac{\partial T}{\partial y} = (T_f - T)h_1 \text{ at } y = 0, \\ u \to u_e = cx,\ N \to 0,\ T \to T_\infty \text{ when } y \to \infty. \end{aligned}\right\} \tag{5}$$

where g denotes the gravitational acceleration, u, v the velocity components, u_e the free stream velocity, x, y the Cartesian coordinates, ρ_{nf} the density, κ^* the vortex viscosity, μ_{nf} dynamic viscosity, σ_{nf} the electrical conductivity, N the micro-rotation vector, B_0 strength of magnetic field, β_1 the thermal expansion coefficient, T the temperature, ν_{nf} kinematic viscosity, T_∞ the ambient temperature, K^* the permeability of porous space, $F\left(=\frac{C_b}{xK^{*\frac{1}{2}}}\right)$ the non-uniform inertia coefficient, γ_{nf} spin gradient viscosity, σ^o Stefan-Boltzman constant, C_b the drag coefficient, j micro-rotation density, c_p specific heat, k_{nf} thermal conductivity, k° the Stefan-Boltzman constant, T_f the fluid temperature, m_0 is the constant $(0 \le m_0 \le 1)$ and h_1 convective heat transfer coefficients. Note that $y = 0$ represents the surface of sheet and *nf* stands for nanofluid. Considering

$$\left.\begin{aligned} \eta = y\sqrt{\frac{a}{\nu_f}},\ u = axf'(\eta),\ v = -\sqrt{a\nu_f}f(\eta),\ N = ax\sqrt{\frac{a}{\nu_f}}g(\eta), \\ \theta(\eta) = \frac{T-T_\infty}{T_f - T_\infty}. \end{aligned}\right\} \tag{6}$$

We arrive to the following dimensionless equations

$$\left.\begin{aligned} \left(\frac{1}{(1-\varphi)^{5/2}} + K_1\right)f''' + \left(1-\varphi+\frac{\rho_s}{\rho_f}\varphi\right)(ff'' - f'^2 + A^2) \\ + K_1 g' - \frac{\sigma_{nf}}{\sigma_f}M(f'-A) - \frac{\beta}{(1-\varphi)^{5/2}}(f'-A) \\ - F_r(f'^2 - A^2) + \lambda\theta\left(1-\varphi+\frac{(\rho\beta_1)}{(\rho\beta_1)_f}\varphi\right) = 0, \end{aligned}\right\} \tag{7}$$

$$\begin{aligned} g''\left(\frac{1}{(1-\varphi)^{5/2}} + \frac{K_1}{2}\right) + \left(1-\varphi+\frac{\rho_s}{\rho_f}\varphi\right)fg' \\ - \left(1-\varphi+\frac{\rho_s}{\rho_f}\varphi\right)f'g - K_1(2g + f'') = 0, \end{aligned} \tag{8}$$

$$\begin{aligned} \frac{1}{\Pr}\left(\frac{k_s + 2k_f - 2\varphi(k_f - k_s)}{k_s + 2k_f + \varphi(k_f - k_s)} + R\right)\theta'' \\ + \left(1-\varphi+\frac{(\rho c_p)_s}{(\rho c_p)_f}\varphi\right)f\theta' = 0, \end{aligned} \tag{9}$$

$$\left.\begin{aligned} f'(0) = 1 + L_1 f''(0),\ f(0) = 0,\ g(0) = -m_0 f''(0), \\ \theta'(0) = -B_1(1-\theta(0)),\ f'(\infty) = A,\ g(\infty) = 0,\ \theta(\infty) = 0. \end{aligned}\right\} \tag{10}$$

Note that, $K_1\left(=\frac{\kappa^*}{\mu_f}\right)$ signifies the micropolar fluid parameter or micro-rotation parameter, $A\left(=\frac{c}{a}\right)$ the velocity ratio or stretching parameter, $M\left(=\frac{\sigma_f B_0^2}{\rho_f a}\right)$ the magnetic variable, $\lambda\left(=\frac{Gr}{\mathrm{Re}^2}\right)$ the mixed convection variable, $\beta\left(=\frac{\nu_f}{K^* a}\right)$ the porosity parameter, $F_r\left(=\frac{C_b}{K^{*\frac{1}{2}}}\right)$ the Darcy Forcheimmer number, $\mathrm{Pr}\left(=\frac{\rho c_p \nu_f}{k_f}\right)$ the Prandtl number, $R\left(=\frac{16\sigma^* T_\infty^3}{3k^* k_f}\right)$ radiation parameter, $L_1\left(=\gamma_1\sqrt{\frac{a}{\nu_f}}\right)$ slip parameter and $B_1\left(=\frac{h_1}{k_f}\sqrt{\frac{\nu_f}{a}}\right)$ thermal Biot number.

The characteristics of nanofluids are defined by [27]:

$$\nu_{nf}=\frac{\mu_f}{(1-\varphi)^{2.5}\left[(1-\varphi)\rho_f+\varphi\rho_s\right]}, \tag{11}$$

$$\rho_{nf}=(1-\varphi)\rho_f+\varphi\rho_s, \tag{12}$$

$$(\rho c_p)_{nf}=(1-\varphi)(\rho c_p)_f+\varphi(\rho c_p)_s, \tag{13}$$

$$(\rho\beta_1)_{nf}=(1-\varphi)(\rho\beta_1)_f+\varphi(\rho\beta_1)_s, \tag{14}$$

$$\frac{k_{nf}}{k_f}=\frac{(k_s+2k_f)-2\varphi(k_s-k_f)}{(k_s+2k_f)+\varphi(k_s-k_f)}, \tag{15}$$

$$\gamma_{nf}=\left(\mu_{nf}+\frac{\kappa^*}{2}\right)j, \tag{16}$$

$$\frac{\sigma_{nf}}{\sigma_f}=\left[1+\frac{3(\sigma-1)\varphi}{(\sigma-2)-(\sigma-1)\varphi}\right]. \tag{17}$$

3. Engineering Curiosity

Mathematically, we have

$$C_{fx}=\frac{2\tau_w}{\rho_f u_w^2}, \tag{18}$$

$$Nu_x=\frac{xq_w}{k_f(T_f-T_\infty)}, \tag{19}$$

in the above equations τ_w denotes the shear stress and q_w the heat flux and defined as

$$\tau_w=(\mu_{nf}+\kappa^*)\left.\frac{\partial u}{\partial y}\right|_{y=0}+\kappa^* N\big|_{y=0}, \tag{20}$$

$$q_w=-k_{nf}\left.\frac{\partial T}{\partial y}\right|_{y=0}+(q_r). \tag{21}$$

In dimensionless form, we arrive

$$\frac{1}{2}C_{fx}\,\mathrm{Re}^{\frac{1}{2}}=\left[\frac{1}{(1-\varphi)^{2.5}}+K(1-m_0)\right]f''(0), \tag{22}$$

$$Nu_x\,\mathrm{Re}^{-0.5}=-\left(\frac{k_{nf}}{k_f}+R\right)\theta'(0), \tag{23}$$

where $\mathrm{Re}\left(=\frac{ax^2}{\nu_f}\right)$ highlights the local Reynolds number.

4. Discussion

Numerical analyses are carried out to find the impact of pertinent flow parameters on the magnetized Darcy-Forchheimer stagnation point flow of non-Newtonian Ferrosoferric Oxide liquid with the convective boundary condition and velocity slip towards a stretched surface of the sheet. The governing Eqs. (1-4) are first altered into ordinary differential Eqs. (7-9) with the help of appropriate similarity transformations (6) and then numerical outcomes are found out through Built-in-Shooting method. The numerical outcomes are organized at a nanoparticle volume fraction (Fe_3O_4) of 0.01 to 0.09 %. Besides, the density, specific heat, thermal conductivity and magnetic field strength of Ferrosoferric Oxide fluid are 5180, 670, 9.7 and 25000 respectively.

The behaviors of important flow parameters on the velocity field, skin friction coefficient, temperature field and Nusselt number are discussed and plotted graphically through Figs. 1-8 and Tables 2 and 3. Table 1 signifies the thermo-physical characteristics of Ferrosoferric Oxide (Fe_3O_4) and water i.e., thermal conductivity, density, magnetic field strength and specific heat. Table 2 depicts the numerical results for skin friction coefficient versus micropolar fluid parameter or micro-rotation parameter, magnetic parameter, Darcy-Forchheimer number and mixed convection parameter. From Table 2, it is witnessed that

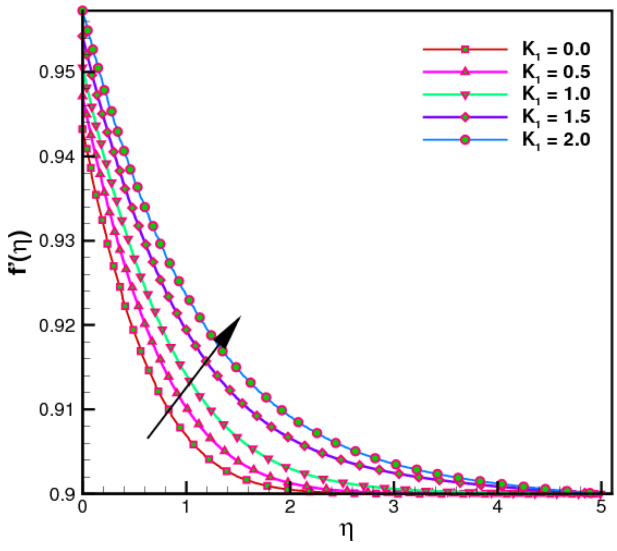

Fig. 1. (Color online) $f'(\eta)$ *versus* K_1.

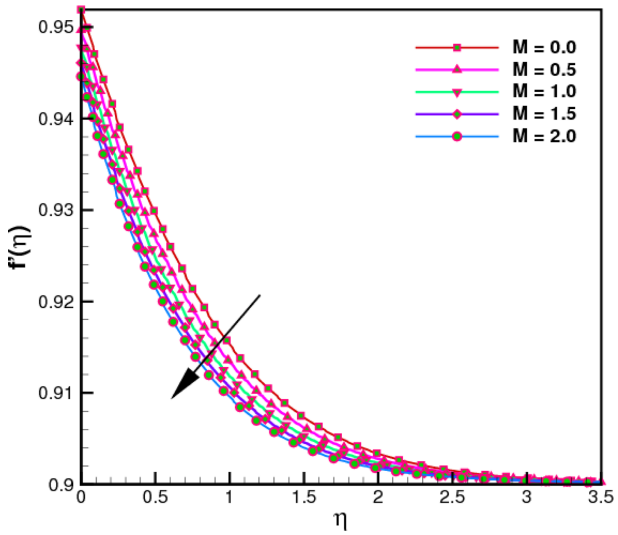

Fig. 2. (Color online) $f'(\eta)$ *versus* M.

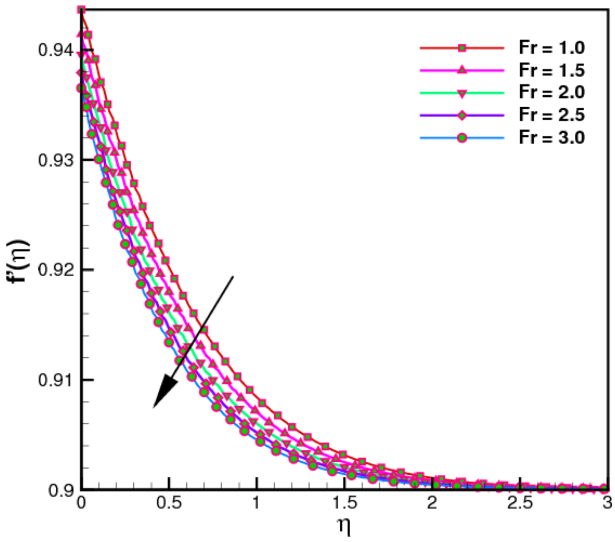

Fig. 4. (Color online) $f'(\eta)$ *versus* Fr.

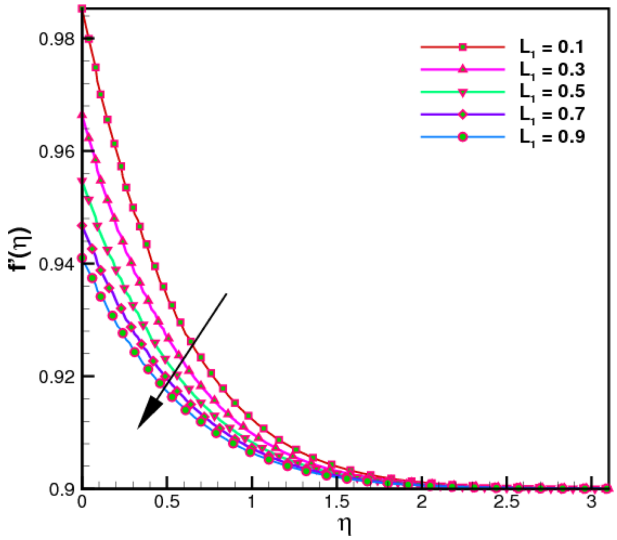

Fig. 3. (Color online) $f'(\eta)$ *versus* L_1.

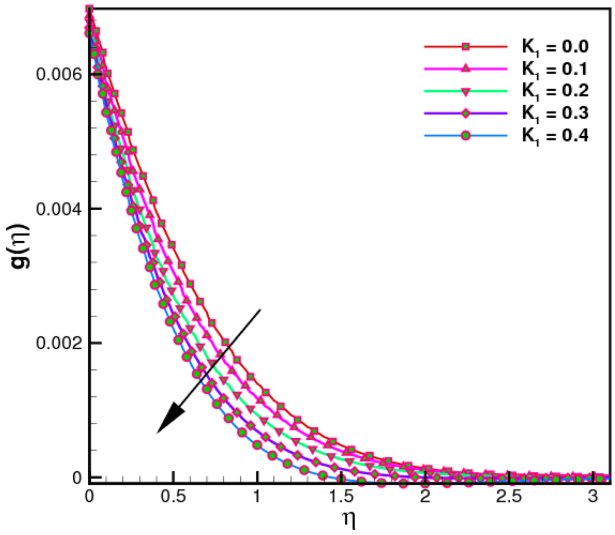

Fig. 5. (Color online) $f'(\eta)$ *versus* A.

magnitude of $C_{fx}\mathrm{Re}^{0.5}$ increases versus micropolar fluid parameter or micro-rotation parameter, magnetic parameter and Darcy-Forchheimer number while declines against higher estimations of mixed convection parameter. Table 3 portrays the physical significance of the Nusselt number versus radiation parameter and thermal Biot number. It is noted that the magnitude of $Nu_x\mathrm{Re}^{-0.5}$ upsurges versus both parameters.

Figure 1 shows the salient aspects of microolar fluid parameter or micro-rotation parameter K_1 = 0.0, 0.5, 1.0, 1.5, 2.0 on the velocity. Velocity profile declines versus rising values of micropolar fluid parameter. Figs. 2 and 3 illustrate the behaviors of magnetic parameter M = 0.0, 0.5, 1.0, 1.5, 2.0 and velocity slip parameter L_1 = 0.1, 0.3, 0.5, 0.7, 0.9 on the velocity field. Here velocity field is a decreasing function of both velocity slip parameter and magnetic parameter. Physically, in Fig. 2, more Lorentz force creates inside the working fluid which oppose the fluid motion and as a result velocity of fluid declines. In Fig. 3, the deformation from the sheet surface is partially transmitted towards the fluid. That's why the velocity decreases. The velocity field versus Darcy-Forchheimer number Fr = 1.0, 1.5, 2.0, 2.5, 3.0 has been displayed in Fig. 4. As is observed, the velocity field decays versus for rising Darcy-Forchheimer number. Physically, the more resistive force created in the working material and consequently the velocity diminish. In Fig. 5, the velocity field has been discussed, subject to velocity ratio parameter A = 0.8, 0.9, 1.0, 1.1, 1.2. From this Fig., it is observed that the velocity of material particles upsurge versus

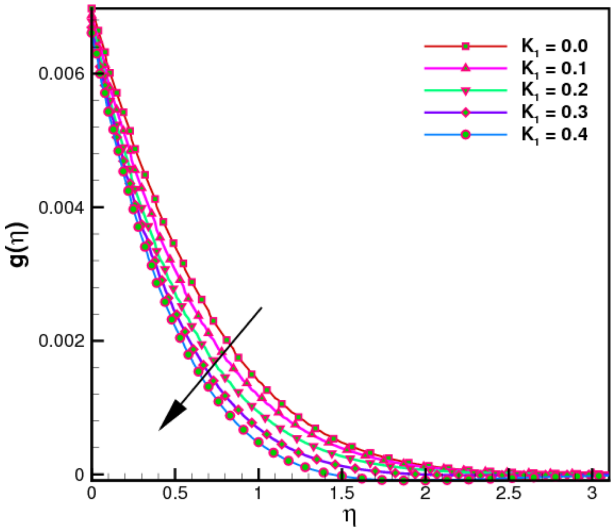

Fig. 6. (Color online) $g(\eta)$ *versus* K_1.

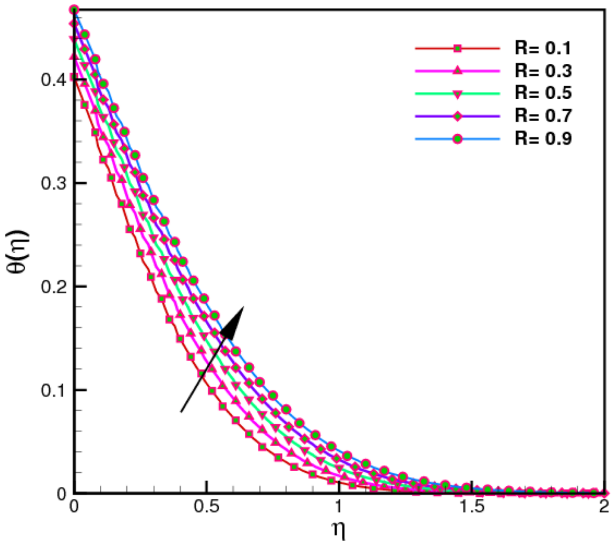

Fig. 7. (Color online) $\theta(\eta)$ *versus* K_1.

Table 1. Various thermo-physical attributes of Ferrosoferric Oxide (Fe_3O_4) and water.

	ρ (kg/m^3)	c_p (J/kgK)	k (W/mk)	σ (Ωm)$^{-1}$
Fe_3O_4	5180	670	9.7	25000
H_2O	997.1	4179	0.613	0.05

larger velocity ratio parameter. There are three different cases, case I: when $A = 1$, there is no boundary layer formation in the fluid, because the sheet the fluid move at the same velocity, case II: when $A > 1$, the sheet and material particles moves with different velocities, i.e., the velocity of material particles is more as compared to sheet velocity, case III: when $A < 1$, the velocity of material particles is less than the sheet velocity. Fig. 6 depicts the

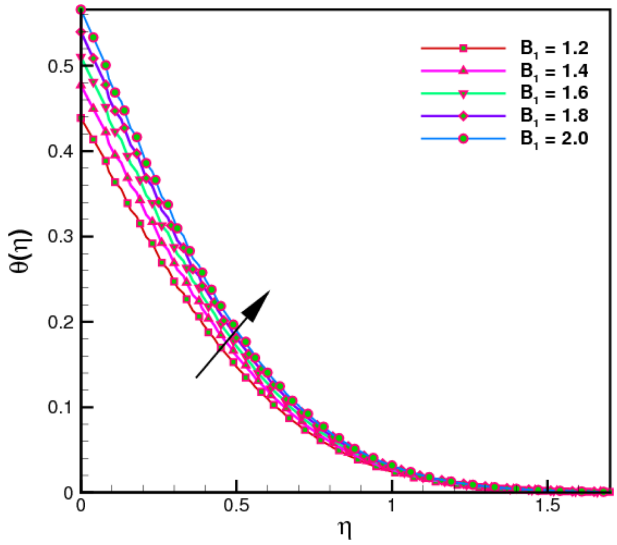

Fig. 8. (Color online) $\theta(\eta)$ *versus* B_1.

Table 2. Computational analysis of skin friction versus various flow parameters.

K_1	M	Fr	λ	$-\frac{1}{2}C_{fx}\mathrm{Re}^{0.5}$
0.5	0.3	1.1	0.1	0.09844
0.6				0.1031
0.7				0.1078
0.8				0.1122
	0.4			0.09889
	0.5			0.09932
	0.6			0.09975
		1.2		0.09992
		1.3		0.09993
		1.4		0.1006
			0.2	0.09361
			0.3	0.08881
			0.4	0.08403
			0.5	0.07928

Table 3. Computational analysis of Nusselt number versus various flow parameters.

R	B_1	$Nu_x\mathrm{Re}^{-0.5}$
0.2		0.837
0.3		0.8902
0.4		0.9423
0.5		0.9934
	1.2	0.8817
	1.3	0.9234
	1.4	0.9625
	1.5	0.9991

variation of velocity ($g(\eta)$) with various estimations of micropolar fluid parameter or micro-rotation fluid para-

meter K_1 = 0.0, 0.1, 0.2, 0.3, 0.4. It is noted that the velocity field is decreasing function of micro-rotation parameter. In Figs. 7 and 8, temperature distribution is discussed for rising estimations of radiation parameter R = 0.1, 0.3, 0.5, 0.7, 0.9 and thermal Biot number B_1 = 1.2, 1.4, 1.6, 1.8, 2.0. Here temperature distribution is an increasing function of both thermal Biot number and radiation parameter.

5. Conclusions

In this communication, we have thoroughly investigated the magnetized flow of micropolar Ferrosoferric Oxide fluid towards a stretched surface under the impact of Lorentz force (magnetic field). Ferrofluids are made out of nanoscale ferromagnetic materials suspended in a base fluid (oil, kerosene, water). The governing expressions are first altered into ordinary ones with the help of appropriate similarity transformations and then numerical outcomes are found out through Built-in-Shooting method. Some important results which are obtained from the communication are listed as:

The fluid velocity $f'(\eta)$ boosts against higher values of micropolar fluid parameter or micro-rotation parameter.

The effects of magnetic parameter, velocity slip parameter and Darcy-Forchheimer number on the velocity field are same. All of these variables decline the velocity field.

The temperature distribution is augmented against radiation parameter and thermal Biot number.

The rate of heat transport slows down via larger values of thermal Biot number while boosting against radiation parameter.

The magnitude of skin friction coefficient upsurges with the increasing values of micropolar fluid parameter or micro-rotation parameter, magnetic parameter, Darcy-Forchheimer number.

Acknowledgments

The research was supported by the National Natural Science Foundation of China (Grant Nos. 11971142, 11871202, 61673169, 11701176, 11626101, 11601485).

References

[1] S. U. S. Choi, Enhancing thermal conductivity of fluids with nanoparticles, Argonne National Lab., IL (United States), Tech. Rep., 1995.
[2] S. Adam and K. N. Premnath, J. Non-Newtonian Fluid Mech. **274**, 104188 (2019).
[3] T. Hayat, M. I. Khan, M. Farooq, A. Alsaedi, M. Waqas, and T. Yasmeen, Int. J. Heat Mass Transf. **99**, 702 (2016).
[4] M. I. Khan, M. Waqas, T. Hayat, and A. Alsaedi, J. Colloid Interface Sci. **498**, 85 (2017).
[5] Q. Du and Q. Gao, J. Magn. **24**, 10 (2019).
[6] M. I. Khan, S. Qayyum, S. Kadry, W. A. Khan, and S. Z. Abbas, J. Magn. **25**, 8 (2020).
[7] Y. S. Daniel, Z. A. Aziz, Z. Ismail, and F. Salah, Alex. Eng. J. **57**, 2187 (2018).
[8] T. Hayat, S. Ahmad, M. I. Khan, and A. Alsaedi, Physica B: Cond. Matt. **537**, 116 (2018).
[9] S. A. Mohammadein, K. Raslan, M. S. Abdel-Wahed, and E. M. Abedel-Aal, Results Phys. **10**, 194 (2018).
[10] A. Riaz, A. Zeeshan, S. Ahmad, A. Razaq, and M. Zubair, J. Magn. **24**, 62 (2019).
[11] T. Hayat, M. I. Khan, A. Alsaedi, and M. I. Khan, Int. Commu. Heat Mass Transf. **89**, 190 (2017).
[12] S. K. Asha and C. K. Deepa, Results Eng. **3**, 100024 (2019).
[13] R. Muhammad, M. I. Khan, N. B. Khan, and M. Jameel, Comput. Meth. Prog. Biomed. **189**, 10529 (2020).
[14] A. R. Hassan, Appl. Math. Comput. **369**, 124843 (2020).
[15] R. Muhammad, M. I. Khan, M. Jameel, and N. B. Khan, Comput. Meth. Prog. Biomed. **188**, 105298 (2020).
[16] Z. Xie and Y. Jian, Int. J. Heat Mass Transf. **127**, 600 (2018).
[17] M. I. Khan, F. Alzahrani, and A. Hobiny, J. Mater. Resear. Techn. **9**, 7335 (2020).
[18] M. P. Boruah, S. Pati, and P. R. Randive, Int. J. Heat Mass Transf. **137**, 138 (2019).
[19] G. J. Reddy, B. Kethireddy, M. Kumar, and M. M. Hoque, J. Mol. Liq. **252**, 245 (2018).
[20] S. Z. Abbas, W. A. Khan, S. Kadry, M. I. Khan, M. Waqas, and M. I. Khan, Comput. Meth. Prog. Biomed. **190**, 105363 (2020).
[21] N. V. Ganesh, Q. M. Al-Mdallal, and A. J. Chamkha, Case Stud. Thermal Eng. **13**, 100376 (2019).
[22] S. Z. Abbas, M. I. Khan, S. Kadry, W. A. Khan, M. Israr-Ur-Rehman, and M. Waqas, Comput. Meth. Prog. Biomed. **190**, 105362 (2020).
[23] M. Kiyasatfar, Int. J. Thermal Sci. **128**, 15 (2018).
[24] M. G. Sobamowo and A. T. Akinshilo, J. Mol. Liq. **241**, 188 (2017).
[25] M. I. Khan and F. Alzahrani, Int. J. Modern Phys. B **34**, 2050132 (2020).
[26] M. Irfan, W. A. Khan, M. Khan, and M. M. Gulzar, J. Phys. Chem. Solid. **125**, 141 (2019).
[27] M. Aghamajidi, M. E. Yazdi, S. Dinarvand, and I. Pop, Propul. Power Resear. **7**, 78 (2018).